

# Radio and Sub-mm Considerations for the ACS Ultra Deep Field

15 January, 2003

Anton Koekemoer, Shardha Jogee, Steve Beckwith, Massimo Stiavelli

## 1 Introduction

The ACS Ultra-Deep Field (UDF) will not only provide the deepest look at the universe with HST, but will also serve as an anchor for a wide variety of follow-up observations across the entire spectrum using space-based and ground-based observatories. While many of the new objects revealed by the UDF will be simply too faint for optical/Near-IR spectroscopic follow-up, they will still be readily detectable in the X-ray, Mid- to Far-IR, and sub-mm to centimeter radio wavelength regimes. Here we discuss the issues concerning the field selection parameters for the UDF in terms of allowing optimal follow-up at frequencies in the range  $\sim 1 - 1000$  GHz, thus covering the general range of sub-mm and centimeter-wave radio astronomy.

## 2 Scientific Motivation for Radio Observations of the ACS UDF

Ultra-deep radio surveys already possess several interesting scientific motivations in and of themselves, including constraints on the number counts of star-forming and active galaxies, tracing the luminosity function evolution of various populations, and providing direct measurements of other interesting observables such as the evolution of the radio source size distribution, and cosmological clustering properties of radio sources. Sub-mm surveys can similarly yield valuable constraints on the evolution of star-formation as traced by dust emission. Moreover, the information provided by such surveys becomes even more valuable when combined with information from other wavelengths, thus we provide here a few examples of interesting science that will greatly benefit from such multiwavelength coverage:

- *Directly tracing radio synchrotron emission from star-forming regions up to the early universe.* The dominant emission mechanism at centimeter wavelengths is the continuum emission from supernova remnants, which can now be readily observed at high redshifts with dedicated ultra-deep radio surveys. For example, a star-formation rate of only  $10 M_{\odot}/\text{year}$  (eg., M82) has a 20 cm flux density  $\sim 20 \mu\text{Jy}$  at  $z = 1$ ; a more massive starburst (eg.,  $100 M_{\odot}/\text{year}$ ) would have flux densities  $\sim 200, 50, 20, 7 \mu\text{Jy}$  at  $z = 1, 2, 3, 5$  respectively. Ultra-deep surveys ( $\sim 25$  days) with the VLA and ATCA could reach 5-sigma levels  $\sim 7 - 15 \mu\text{Jy}$ , thus currently we have the capability in both hemispheres to detect moderate star-formation up to  $z \sim 1$  and massive starbursts up to  $z \sim 5$ . EVLA is intended to improve the VLA sensitivity by about an order of magnitude, and should thus be able to detect normal star-formation up to  $z \sim 5$ , while more massive starbursts should be detectable well beyond reionization. Combining the radio data with the detailed morphology and colour information obtained from the ACS UDF will yield important information about a range of star-formation indicators that can be directly compared with the FIR/sub-mm dust emission.
- *Probing the cosmological evolution of radio galaxies and quasars.* An important clue for understanding the fundamental nature of the bulge/black-hole mass correlation is provided by active galaxies, since they directly trace black hole properties throughout the history of the universe. Ultra-deep radio data allow constraints to be obtained on the amount of kinetic

energy extracted from black holes via radio jets, while hard X-ray emission traces the direct radiative output from the AGN. Particularly useful for AGN is the ability to study them using VLBI techniques, especially for more compact sources at high redshift. Important recent advances in wide-field VLBI (eg., Garrett et al. 2001) have enabled deep VLBI data to be obtained instantaneously over a sufficiently wide field of view that many sources can be imaged simultaneously to relatively deep levels for VLBI (eg., 5-sigma levels  $\sim 200 \mu\text{Jy}$ ). The resulting detailed information about the AGN and their jets at high redshift, combined with the high-quality ACS morphological information about their hosts, can enable a wide range of studies of how the black hole properties are inter-related to those of the hosts at early epochs.

- *Dust emission and molecular lines at cosmological redshifts.* Perhaps the most exciting possibility is that the high spectral resolution, wide bandwidths and deep sensitivity for the planned upgrades and future generation of radio telescopes will allow direct spectroscopy of a large number of molecular species at redshifts up to 10 or above, thus not only providing the potential to measure redshifts well beyond reionization, but also directly trace the metallicity history of the universe at early epochs.

### 3 Current and Future Ground-Based Radio Telescopes

#### 3.1 Centimeter Wavelengths

The two primary radio synthesis telescopes that can currently achieve the depth, resolution and sensitivity required for ultra-deep centimeter wavelength surveys are the Very Large Array (VLA) and the Australia Telescope Compact Array (ATCA). The VLA has a declination range  $+90$  to  $-40$ , while the ATCA has a declination range  $-20$  to  $-90$  (above  $-20$ , the VLA is more competitive). Both have been used successfully in the past for ultra-deep surveys, typically reaching  $1\text{-}\sigma$  r.m.s.  $\sim 1 - 2 \mu\text{Jy}$  at 3 cm (eg., Fomalont et al. 2002) and  $\sim 8 - 10 \mu\text{Jy}$  at 20 cm (eg., Richards et al. 1998; Hopkins et al. 1998; Kellermann et al. 2000). In Table 1 we summarize their capabilities, showing also the approximate 1-sigma r.m.s. sensitivities for continuum sources after 12 h of integration. For the ATCA, the current sensitivities were calculated utilizing both bandpasses to achieve the maximum bandwidth (2x128MHz). In addition, calculations are given for the ATCA correlator upgrade to 2 GHz instantaneous bandwidth (commenced in April 2002, and scheduled for completion during 2004), enabling sampling of the entire bandpass of each receiver, thereby increasing the sensitivity particularly at shorter wavelengths.

Once the ATCA 2 GHz correlator upgrade is complete (scheduled for 2004), it will have comparable sensitivity to the VLA in the bands that they have in common. Currently the VLA is a factor  $\sim 2$  times more sensitive than the ATCA at most wavelengths, although for southern fields the two instruments become comparable due to the advantages of higher elevations at the ATCA, leading to better phase stability and system temperatures, and higher observing efficiency. The ATCA is also much more efficient at mosaicing than the VLA, and this is even valuable for ultra-deep fields since a compact mosaicing pattern can produce uniform depth over a larger area than a single pointing, and also greatly improve the calibration and removal of sidelobes from sources near the edge of the primary beam, by placing them at the centre of other pointings.

The current ATCA correlator configurations range from 2x128 MHz instantaneous bandwidth (2x32 independent channels, 4 polarizations), to 4 MHz bandwidth with 4096 channels (1 IF, 1 polarization product). The correlator upgrade will provide 2 GHz instantaneous bandwidth (with 512 channels and 4 polarization products), while spectral line observations could use, for example, a 4 MHz bandwidth with 8096 channels and all 4 Stokes products. By comparison, the VLA currently ranges from 50 MHz bandwidth, 4 channels, 4 IFs, to 0.195 MHz, 512 channels, 1 IF. The VLA

Table 1: Comparison of Observational Capabilities of the VLA and ATCA

	Band (cm)	Freq Range (GHz)	Primary Beam (')	Synthesised Beam (")	Tsys (K)	12h r.m.s. (mJy/beam)	
VLA:							
	90	0.303 - 0.34	150	6.0	150 - 180	0.170	
	20	1.17 - 1.74	30	1.4	37 - 75	0.007	
	6	4.25 - 5.10	9	0.4	45	0.006	
	3.6	7.55 - 9.05	5.4	0.24	35	0.005	
	2	14.3 - 15.7	3	0.14	120	0.020	
	1.3	20.6 - 25.2	2	0.08	50 - 80	0.025	
	0.7	39 - 47.5	1	0.05	80	0.030	
ATCA:							
						Current	After 2 GHz upgrade
	20	1.25 - 1.78	33	6	35	0.015	0.010
	13	2.20 - 2.50	22	4	33	0.023	0.021
	6	4.40 - 6.86	10	2	33	0.018	0.006
	3	7.55 - 9.05	5	1	40	0.021	0.008
	1.2	16 - 26	2.5	0.5	75	0.060	0.021
	0.3	84 - 115	0.5	0.1	230	0.390	0.138

retains an advantage in spatial resolution over the ATCA by about a factor  $\sim 4$ . Moreover, the currently planned VLA Expansion (EVLA) will aim to increase continuum sensitivity by a factor  $\sim 5 - 20$ , with a maximum bandpass of 8 GHz and up to 16,384 channels. The project is currently scheduled to be completed by 2009.

### 3.2 Sub-Millimeter and Millimeter Wavelengths

Submm and mm followups of the UDF will trace cold gas and dust in high redshift systems and thereby set constraints on the physical properties of their ISM, their star formation history, chemical evolution, and dynamical masses. Such observations can yield insights into the nature of the large population of dusty submillimeter galaxies that dominate the luminosity of the Universe at high redshift, the starburst–AGN connection, and the symbiotic growth of the bulge and black hole in the centers of galaxies. Table 2 lists capabilities of current and future mm and submm facilities. By 2005–2007, bolometer arrays on single dish telescopes such as BOLOCAM II on the 50m Large Millimeter Telescope (LMT), HAWC on SOFIA (60/110/200  $\mu$ ), SHARC-II on JCMT, SCUBA-II on JCMT will produce wide field submm/mm images whose depth is ultimately set by the confusion limit imposed by the relatively large (7''–15'') beam of the dish. Interferometers such as the Submillimeter Array (SMA), ATCA, the Combined Array for Research in Millimeter-wave Astronomy (CARMA), and the Atacama Large Millimeter Array (ALMA) can filter flux on large scales and will have a deeper confusion limit (Table 2). For a UDF field near the equator, LMT, CARMA, SMA, and ALMA can do efficient followups. For a UDF field at declination of -28 degrees, LMT, ATCA, SMA, and ALMA are alternatives.

**ALMA:** The Atacama Large Millimeter Array (ALMA), a joint U.S. National Radio Astronomy Observatory and European Southern Observatory project, will be a giant step in mm/submm astronomy, providing at least one order of magnitude superior sensitivity and angular resolution (Table 2) compared to existing facilities. Expected to be operational by 2010, ALMA will consist of 64 x 12m antennae at an altitude of 5000m on Chajnantor in Chile, 7238 m<sup>2</sup> of collecting area (1 order of magnitude larger than current interferometers) and baselines typically of 10–12 km long. At typical operating wavelengths (0.35–8.60 mm), the angular resolution (0.006''–0.1'') will match or exceed that of HST, NGST and VLTI. The sensitivity will be at least 2 orders of magnitude superior to that of existing interferometers (Table 2). In 12 hours, ALMA reaches a 1  $\sigma$  continuum r.m.s. of 7, 20, 30, 200  $\mu$ Jy respectively at 3mm, 1.3mm, 870 $\mu$ , and 440 $\mu$  (Table 2).

Table 2: **Current and future ground-based submm/mm facilities**

(1)	(2)	(3)	(4)	(5)	(6)	(7)	(8)	(9)	(10)
$\lambda$	Observ.	Dec	fov	Resol	Tssb	Cont	Cont.	Year	Confusion.
(mm)		( $^{\circ}$ )	( $''$ )	( $''$ )	(K)	BW (GHz)	rms (mJy/bm)		limit (mJy)
3.0	OVRO	-25,+80	65	1.0	300	4	1.2	2003	
3.0	BIMA	-25,+80	115	1.1	300	1.6	1.0	2003	
3.0	PdBI	-25,+80	50	1.2	150	0.58	0.1	2003	
3.0	NMA	-25,+80	68	2.1	500	2.0	0.8	2003	
3.0	ATCA	-90,-20	31	0.4	350	2.1	0.6	2004	
3.0	CARMA	-25,+80	115	0.4	200	8	0.03	2005	
1.3	CARMA	-25,+80	65	0.2	200	8	0.08	2005	
1.3	LMT <sup>a</sup>	-40,+80	720	5	-	70	[9e-3] <sup>b</sup>	2005	6e-3 (4e-5)
1.3	SMA	-40,+80	52	0.5	142	2	0.3	2004	< 1e-9 (< 1e-9)
0.870	SMA	-40,+80	18	0.3	340	2	0.8	2004	< 1e-7 (< 1e-6)
0.450	SMA	-40,+80	52	0.2	2640	2	7.1	2004	< 1e-8 (< 1e-4)
3.0	ALMA	-80,+20	50	0.05	30	16	7e-3	2010	< 1e-9 (< 1e-9)
1.3	ALMA	-80,+20	25	0.02	70	16	0.02	2010	< 1e-9 (< 1e-9)
0.870	ALMA	-80,+20	17	0.01	190	16	0.03	2010	< 1e-7 (< 1e-6)
0.450	ALMA	-80,+20	9	0.006	430 <sup>c</sup>	16	0.2	2010	< 1e-8 (< 1e-4)

Columns : (1) Observing wavelength; (2) Observatory: LMT<sup>a</sup> = with Bolocam II camera; (3) Typical observable declination range; (4) Field of view or half power beam width; (5) Resolution: For interferometers, we give the typical synthesized beam for extragalactic observations and for bolometer camera, the pixel size; (6) Typical zenith Single sideband system temperature. c. For ALMA at 0.450 mm  $T_{\text{sys}} = 450$  K at PWV=0.3 mm and 3500 K at PWV=1.5 mm; (7) Continuum bandwidth; (8) Continuum sensitivity ( $1\sigma$ ) r.m.s. for 12 hrs. Values for interferometers are in mJy/beam except for bolometer cameras (incoherent detectors) where values are in mJy and enclosed in square brackets. (9) Expected year of operation: 2003 indicates existing facility; (10) Confusion limit due to galaxies and due to the ISM in brackets, estimated from Blain et al. 2002.

While performance is marginal near  $440\mu$ , this band is generally not even reachable from current ground-based facilities. The expected flux density of a dusty ( $40\text{ K}$ ,  $10^{10} L_{\odot}$ ) galaxy redshifted to  $z = 1-10$  is 0.1, 2, 5  $\mu\text{Jy}$  respectively at 3.0 mm, 1.4 mm, and  $870\mu$ . For a  $38\text{ K}$ ,  $10^{12} L_{\odot}$  galaxy, corresponding values are 200, 1000, 300  $\mu\text{Jy}$  respectively (see Figure 1). This value is approximately *independent of redshift*, within a factor of 2, due to the *powerful K correction* at  $z = 1-10$  in the submm/mm (300–2100  $\mu$ ) regime. Down to 100  $\mu\text{Jy}$ , the expected number counts of sources per  $\text{deg}^2$  is 300,  $2 \times 10^4$ ,  $8 \times 10^4$  at 3.0 mm, 1.4 mm, and  $850\mu$ , respectively (e.g., Blain et al. 2002).

**LMT:** The 50m single-dish LMT is being jointly built by INAOE in Mexico and the University of Massachusetts in Amherst, and will be located atop Sierra Negra at an altitude of 4600m in Puebla, Mexico. Characteristics of LMT are 1–4 mm operational wavelengths, a collecting area of 2000  $\text{m}^2$  (5 times that of OVRO), multi-pixel cameras (BOLOCAM II at 1 mm with  $144 \times 5''$  pixels and the SEQUOIA camera at 3mm with 16 dual polarization pixels), and a “redshift machine” with a whopping 35 GHz of instantaneous bandwidth. BOLOCAM II on LMT (Table 2) will reach  $1\sigma$  of 0.006 mJy in 1 hr and detect the brightest SCUBA sources in a few seconds, thus giving better performance than SCUBA on the JCMT and MAMBO on the IRAM 30 m. The LMT redshift machine will increase the number ( $\sim 20$ ) of galaxies and QSOs with CO detection substantially: every galaxy at  $z > 2$  in UDF will have at least one CO line falling in the 35 GHz bandwidth since the redshifted ladder of CO lines are separated by  $115/(1+z)$ . Furthermore, the redshift machine

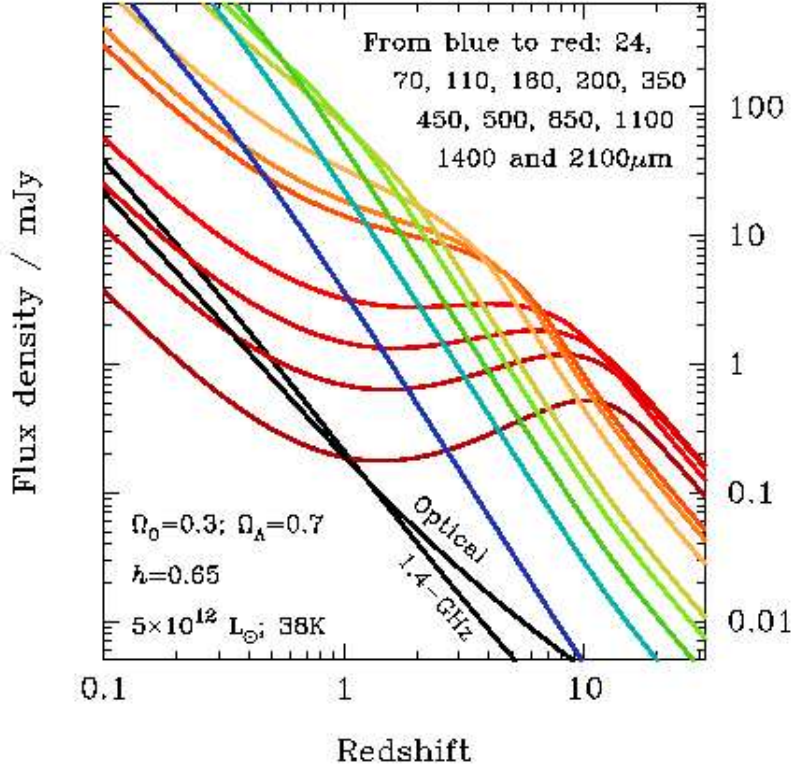


Figure 1: Flux density as a function of redshift, for a range of frequencies.

will be particularly useful for measuring redshifts out to  $z = 6-10$ , where redshifted Ly $\alpha$  passes into the near-IR, making optical redshifts useless. However, like all single dish telescopes, the depth of LMT surveys will be ultimately set by the confusion limit (Table 2) imposed by the large beam size.

**CARMA:** The Universities of California at Berkeley, Illinois, and Maryland, and the California Institute of Technology, are designing and building CARMA. CARMA will merge the six 10.4-m telescopes of Caltech's Owens Valley Radio Observatory (OVRO) mm-wave array and nine 6.1-m telescopes of the Berkeley-Illinois-Maryland Association (BIMA) mm-wave array on a new site at elevation 8000 ft in the Inyo Mountains of California. It is expected that the eight 3.5-m telescopes of the University of Chicago Sunyaev-Zeldovich Array (SZA; J. Carlstrom, P.I.) will also be part of the new array. CARMA, is expected to be operational in 2005 and with this mix of telescope diameters, it will provide high image fidelity over a range of angular scales that make possible wide field imaging and mosaicing, as well as angular resolution to  $0.2''$  at the shortest wavelength. The CARMA 4 GHz COBRA correlator, covering 4% uncertainty in  $z$  will enable followup detection of CO in galaxies with less precisely known redshifts.

## 4 Issues Governing Field Selection

The dynamic range can be limited by strong sources near the steep half-power radius of the primary beam, since random pointing errors can cause amplitude fluctuations and limit the extent to which such sources can be deconvolved. Specifically, the following criteria can be used as guidelines for minimizing problems caused by strong sidelobes at 20 cm:

- no sources brighter than 1 Jy within a 1.5 degree radius
- no sources brighter then 500 mJy within a 1 degree radius

- no sources stronger than 100 mJy within a 0.5 degree radius
- the worst remaining source very near the field center (in order to provide optimum removal of sidelobes).

The CDFS comes close to satisfying the above criteria, since the three strongest sources within a  $35'$  radius from our target center have flux densities of 56, 58 and 93 mJy at 20 cm, although there are some brighter sources further out. To date there have been two deep surveys of the CDFS:

- Kellermann et al. with the VLA, 6 & 18 cm, reaching  $\sim 10 \mu\text{Jy}$  r.m.s. near the field center but with decreased sensitivity at distances further than  $\sim 10'$  since it is only a single pointing;
- Koekemoer et al. with the ATCA, initially at 20 cm aiming to reach depths  $\sim 5 - 10 \mu\text{Jy}$  across the entire XMM field diameter ( $30'$ ) by using a compact mosaicing pattern, and now following up at 3 and 6 cm. See Figure 2 for the preliminary 20 cm map of the CDFS.

In Figures 3 to 12 we display maps of  $10^\circ \times 10^\circ$  regions around ten of the possible deep field candidates that are listed in Table 3 of the document entitled “Field Selection Criteria for the ACS Ultra Deep Field” (Stiavelli et al.), showing the distribution of bright radio sources at 20 cm around each field.

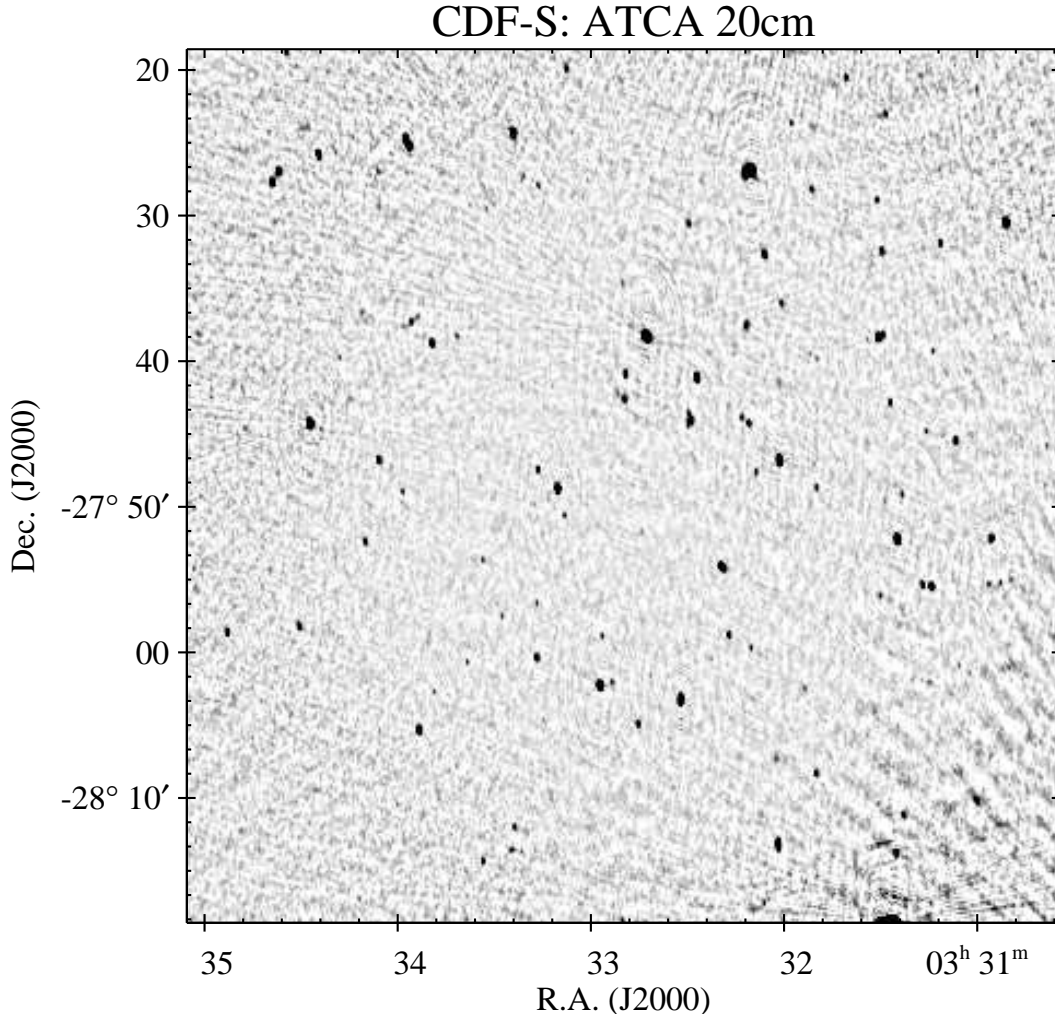


Figure 2: One-degree ATCA map of the CDFS at 20 cm from Koekemoer et al. (2002).

## 5 Summary

A comparison of the current and planned radio/sub-mm telescopes can be summarised as follows:

1. At centimeter wavelengths, the VLA sensitivity will be matched during 2004 by the ATCA 2 GHz correlator upgrade, thus the two instruments will reach similar depths. The VLA in A-array mode retains its spatial resolution advantage of  $\sim 4$  times over the ATCA, making it less susceptible to 20 cm confusion. Its larger number of baselines also make it easier to achieve higher dynamic range.
2. The ATCA retains a wider instantaneous bandwidth and a higher spectral resolution, by  $\sim 4$  times relative to the VLA until the completion of the EVLA upgrade.
3. The EVLA, scheduled for completion during 2009, will increase the sensitivity of the VLA by approximately an order of magnitude at most frequencies, as well as providing a wider bandwidth and more channels.
4. The current generation of millimeter-wave observatories (OVRO, BIMA, PdBI and Nobeyama) will be overtaken by CARMA, SMA and the ATCA in terms of resolution and sensitivity within the next year or two. These will remain the dominant millimeter-wave telescopes until the advent of ALMA.
5. In the sub-millimeter domain, SMA will be the telescope of choice until ALMA is operational.

## Acknowledgements

We are grateful to Ron Ekers, Rogier Windhorst, Frazer Owen, Ed Fomalont, Marijn Franx, and Chris Carilli for valuable feedback and comments that have contributed to this discussion.

## References

- Carilli, C. L. 2000, astro-ph/0011199
- Fomalont, E. B., Kellermann, K. I., Partridge, R. B., Windhorst, R. A., & Richards, E. A. 2002, AJ, 123, 2402
- Garrett, M. A., Muxlow, T. W. B., Garrington, S. T., Alef, W., Alberdi, A., van Langevelde, H. J., Venturi, T., Polatidis, A. G., Kellermann, K. I., & Baan, W. A., 2001, A&A, 366, L5
- Hopkins, A. M., Mobasher, B., Cram, L., & Rowan-Robinson, M., 1998, MNRAS 296, 839
- Kellermann, K. I., Fomalont, E. B., Rosati, P., & Shaver, P., 2000, BAAS 197, 9002
- Koekemoer, A. M., Mobasher, B., Afonso, J., Chan, B., Conselice, C., Cram, L., Grogin, N. A., Jackson, C., Joglee, S., Lucas, R., Norris, R. P., Padovani, P., Schreier, E. J., Chatzichristou, E., Urry, M., Fosbury, R., & Etori, S., 2003, AAS 201, 0602
- Richards, E. A., Kellermann, K. I., Fomalont, E. B., Windhorst, R. A., & Partridge, R. B., 1998, AJ 116, 1039

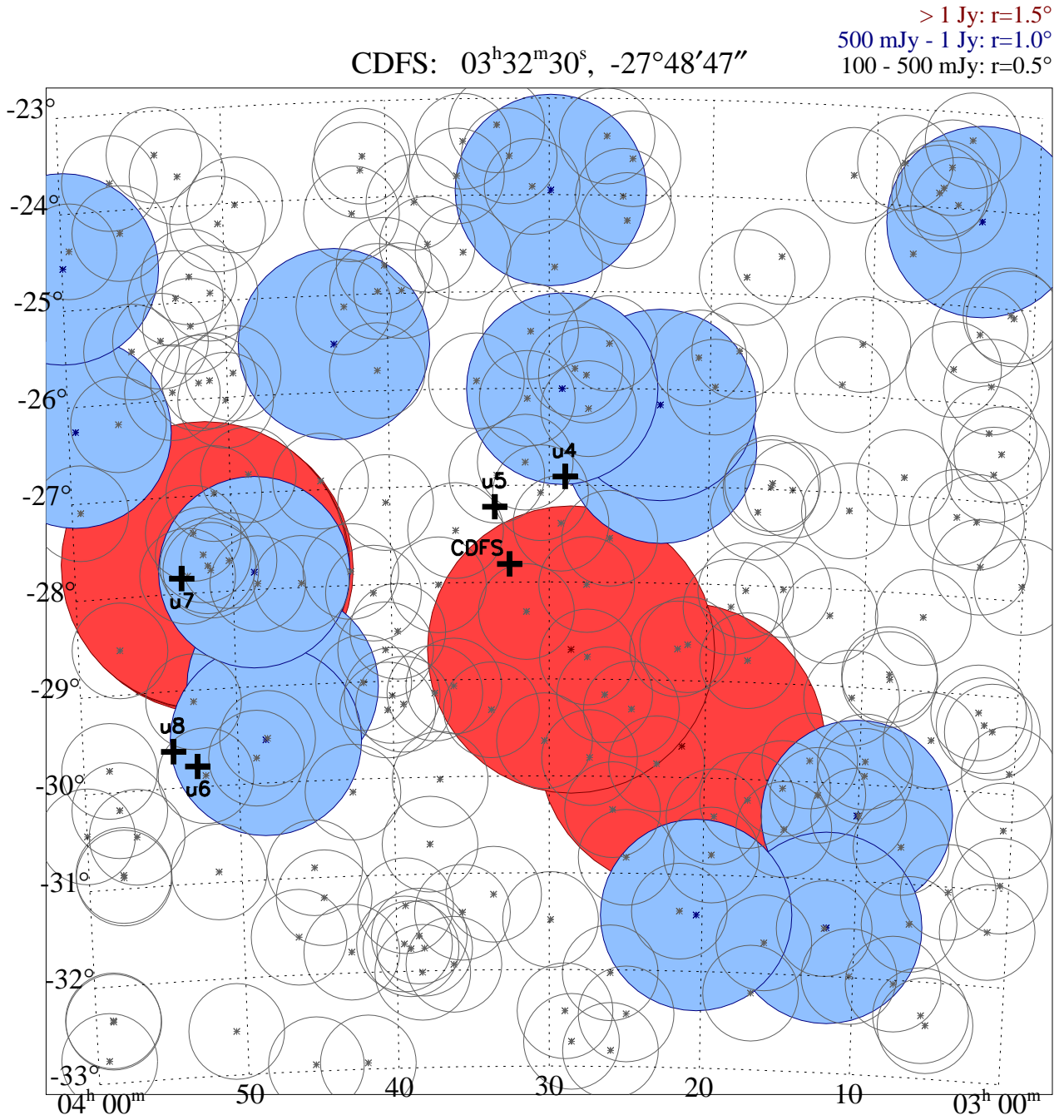


Figure 3: Region covering  $10^{\circ} \times 10^{\circ}$  around the CDFS, showing the distribution of NVSS sources brighter than 100 mJy at 20 cm, along with the sizes of regions to be avoided around these sources. The largest circles (in red) indicate regions 3 degrees in diameter, to be avoided around sources with a 20 cm flux density of 1 Jy or brighter. Smaller circles (in blue) indicate regions 2 degrees across, to be avoided around sources with 20 cm flux densities in the range 0.5 – 1 Jy. The remainder of the circles indicate regions 1 degree in diameter, to be avoided around sources with flux densities between 100 – 500 mJy at 20 cm. We also indicate the location of the CDFS field center, as well as the fields ‘u4’, ‘u5’, ‘u6’, ‘u7’ and ‘u8’ that are listed in Table 3 of the document entitled “Field Selection Criteria for the ACS Ultra Deep Field” (Stiavelli et al.)



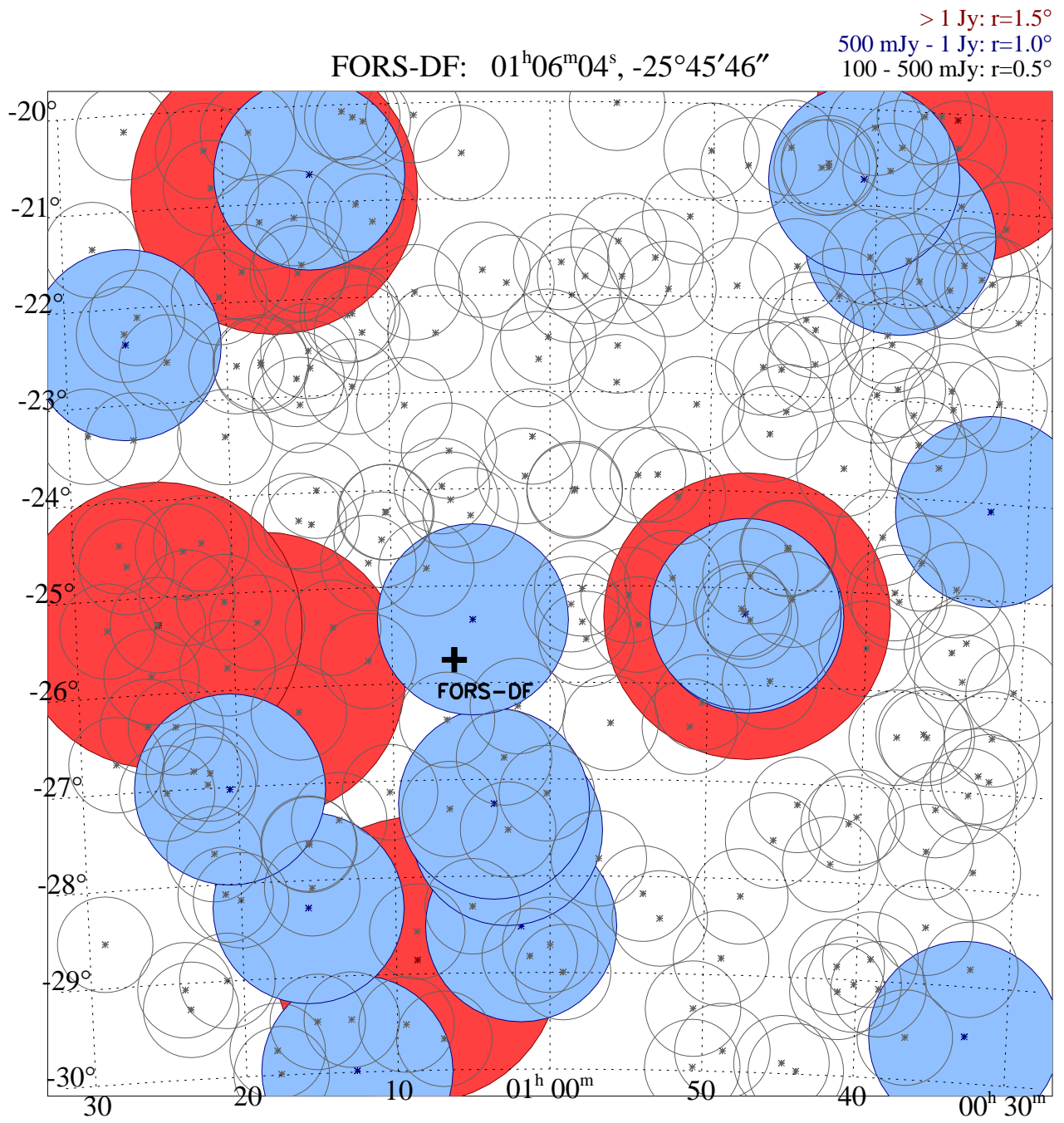


Figure 4: As for Figure 3, but for the FORS Deep Field.

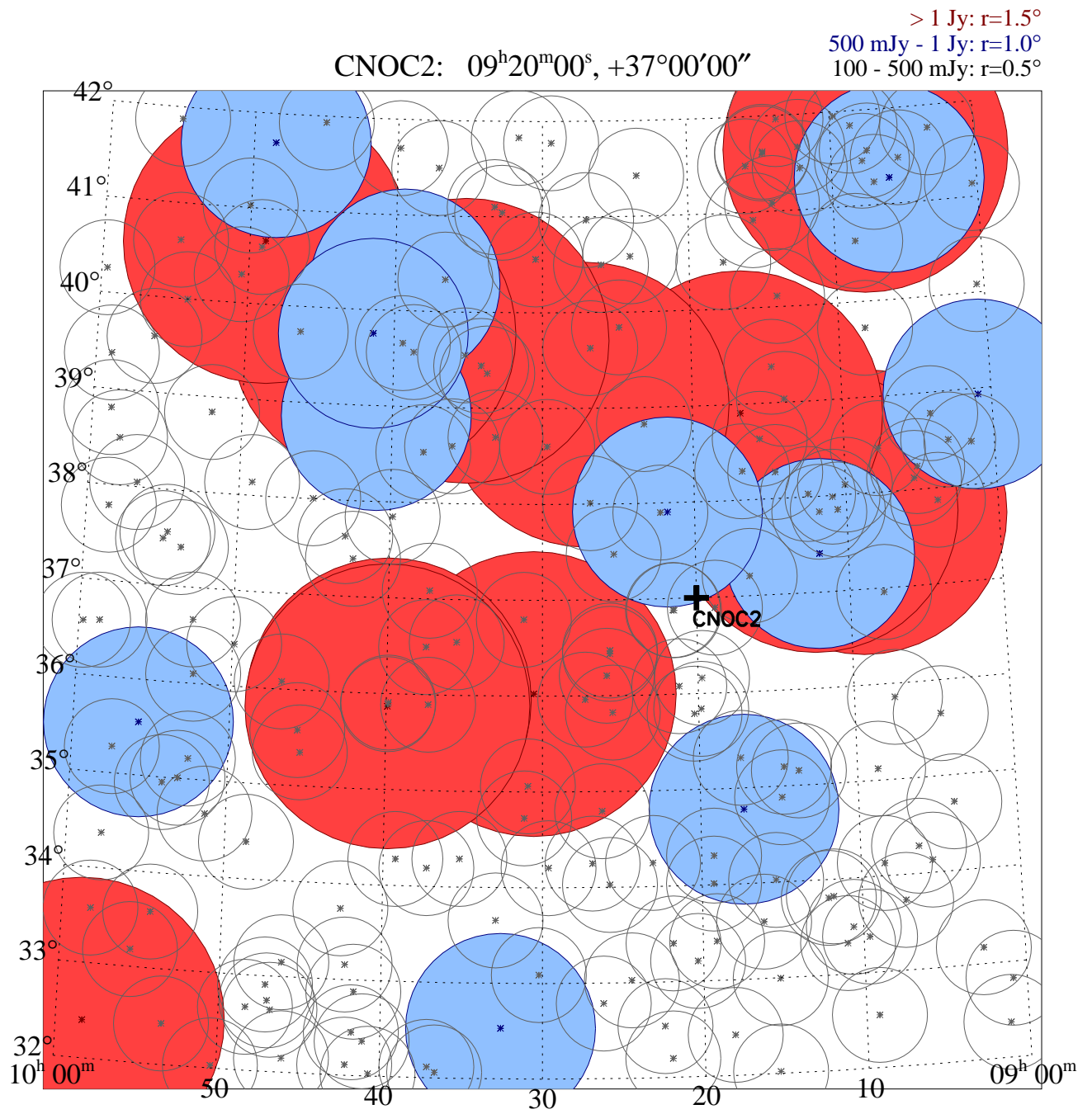


Figure 5: As for Figure 3, but for the CNOC2 field.

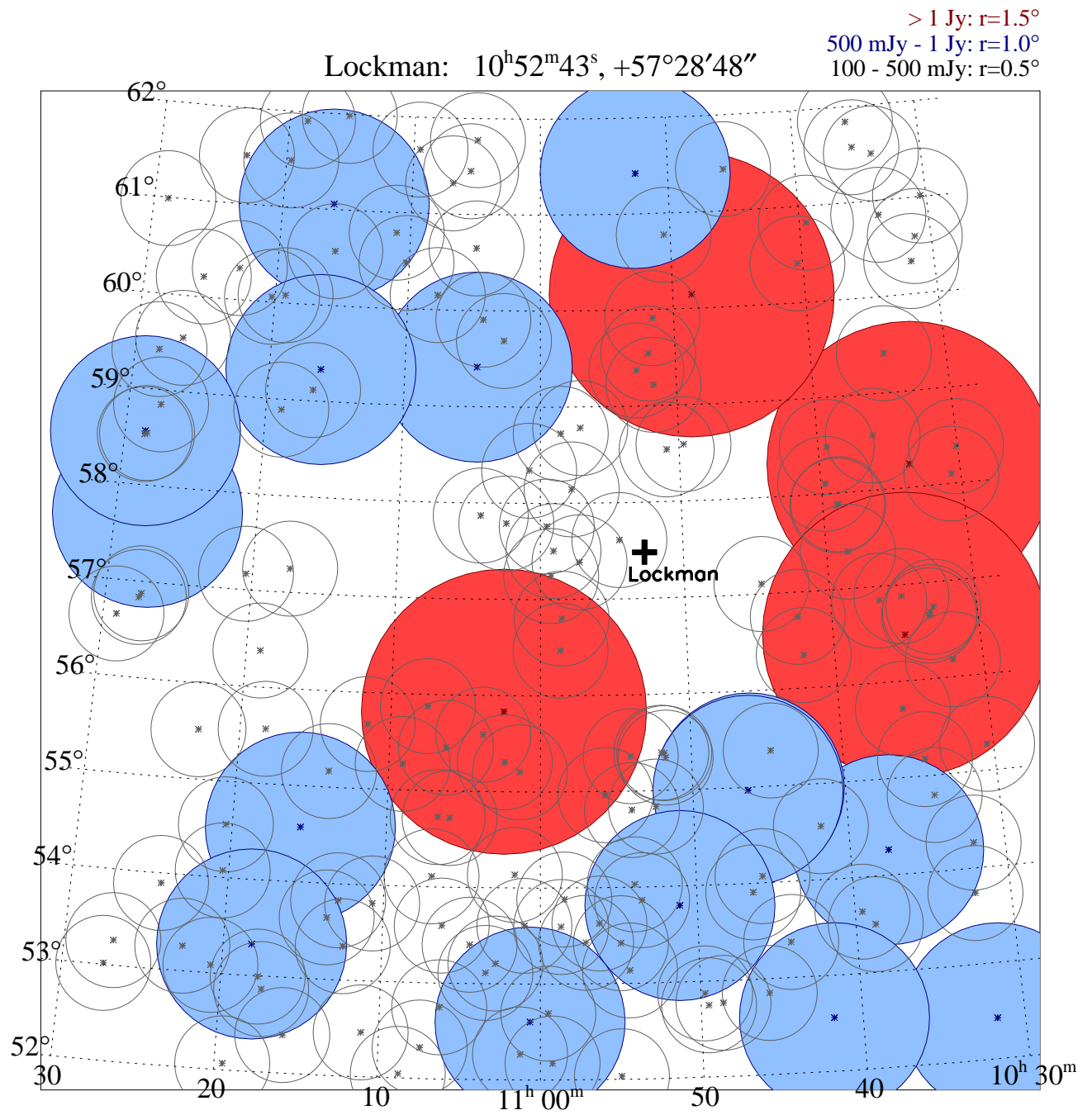


Figure 6: As for Figure 3, but for the Lockman hole.

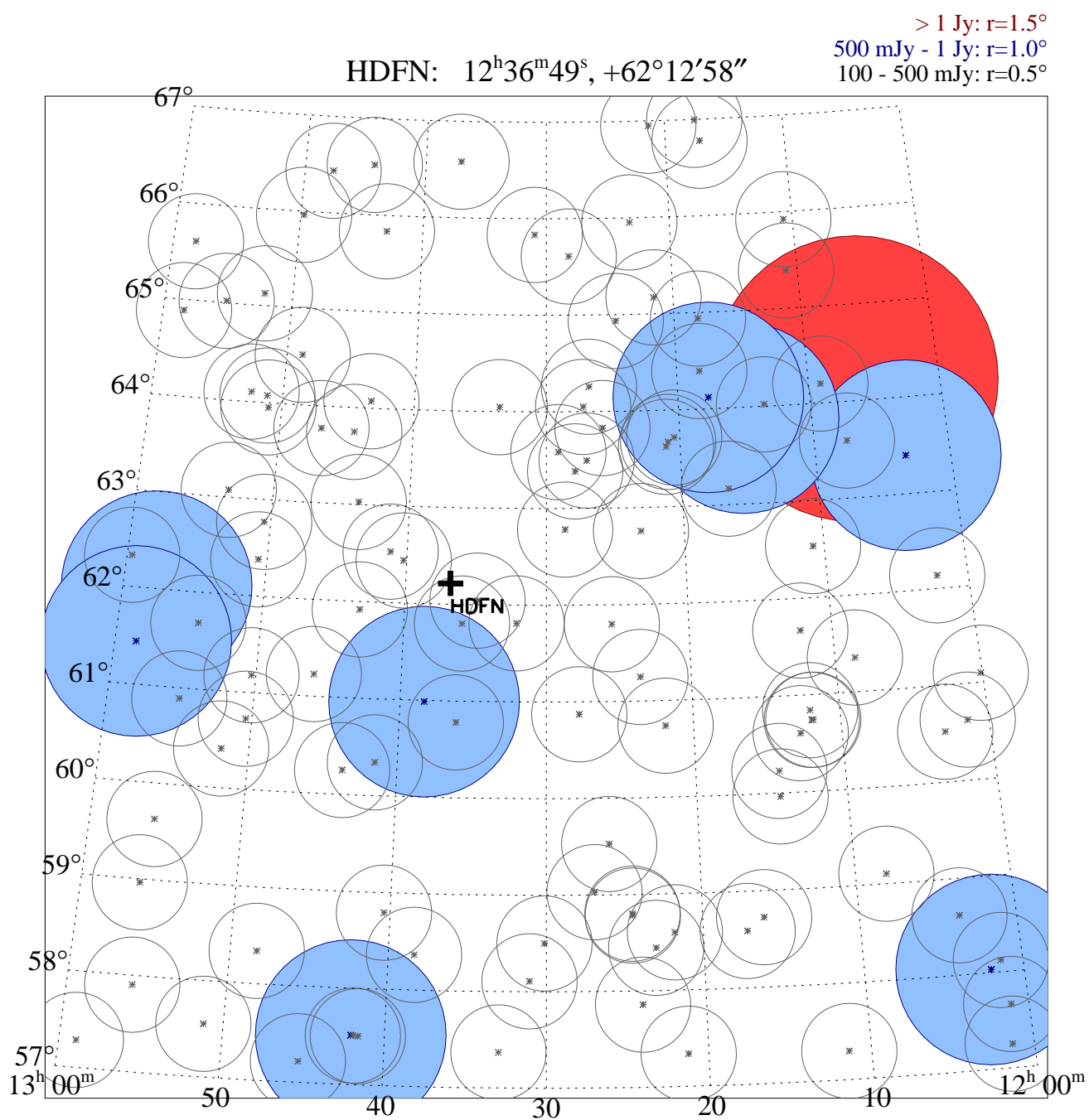


Figure 7: As for Figure 3, but for the HDF-N.

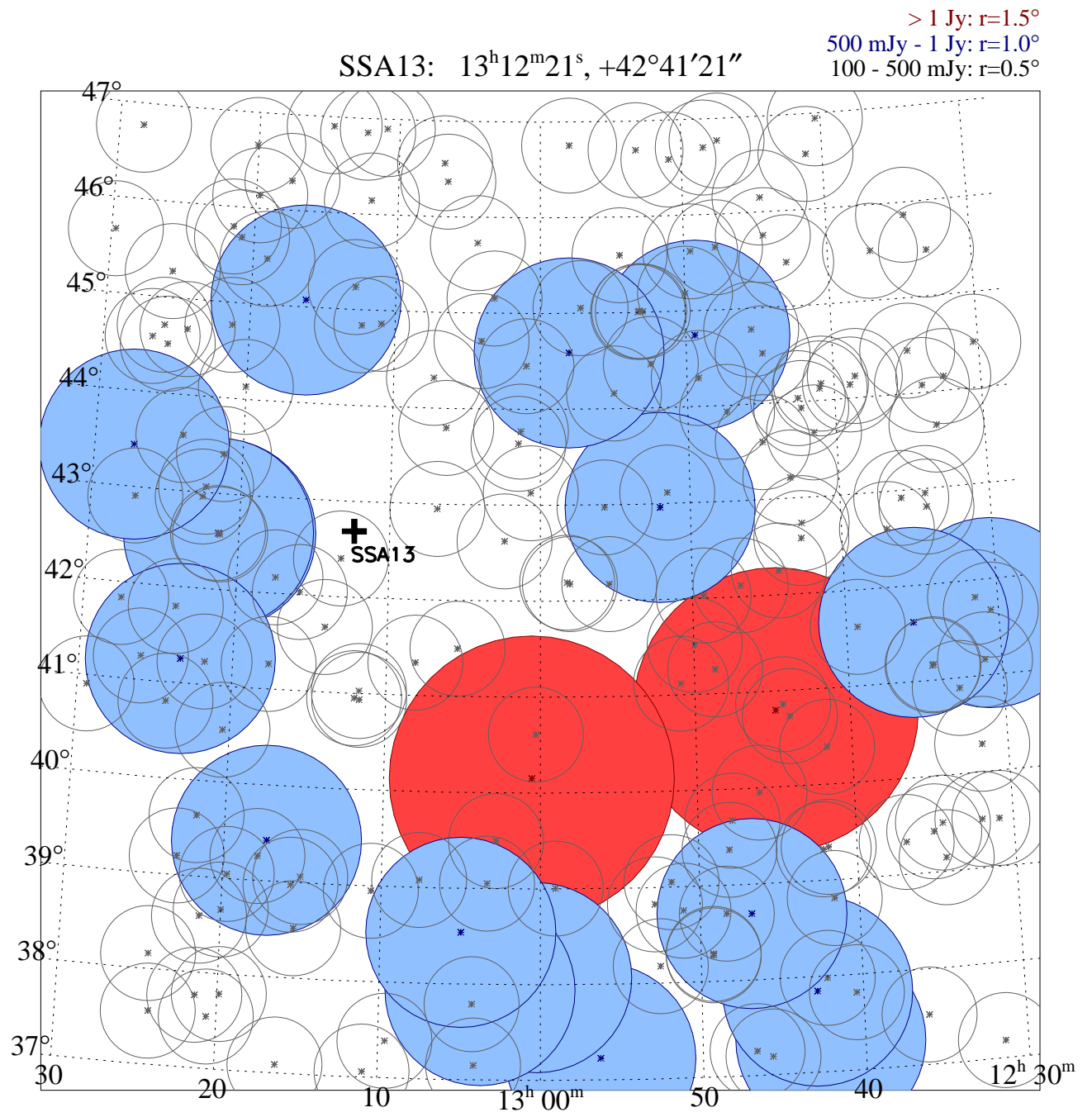


Figure 8: As for Figure 3, but for the SSA13 field.



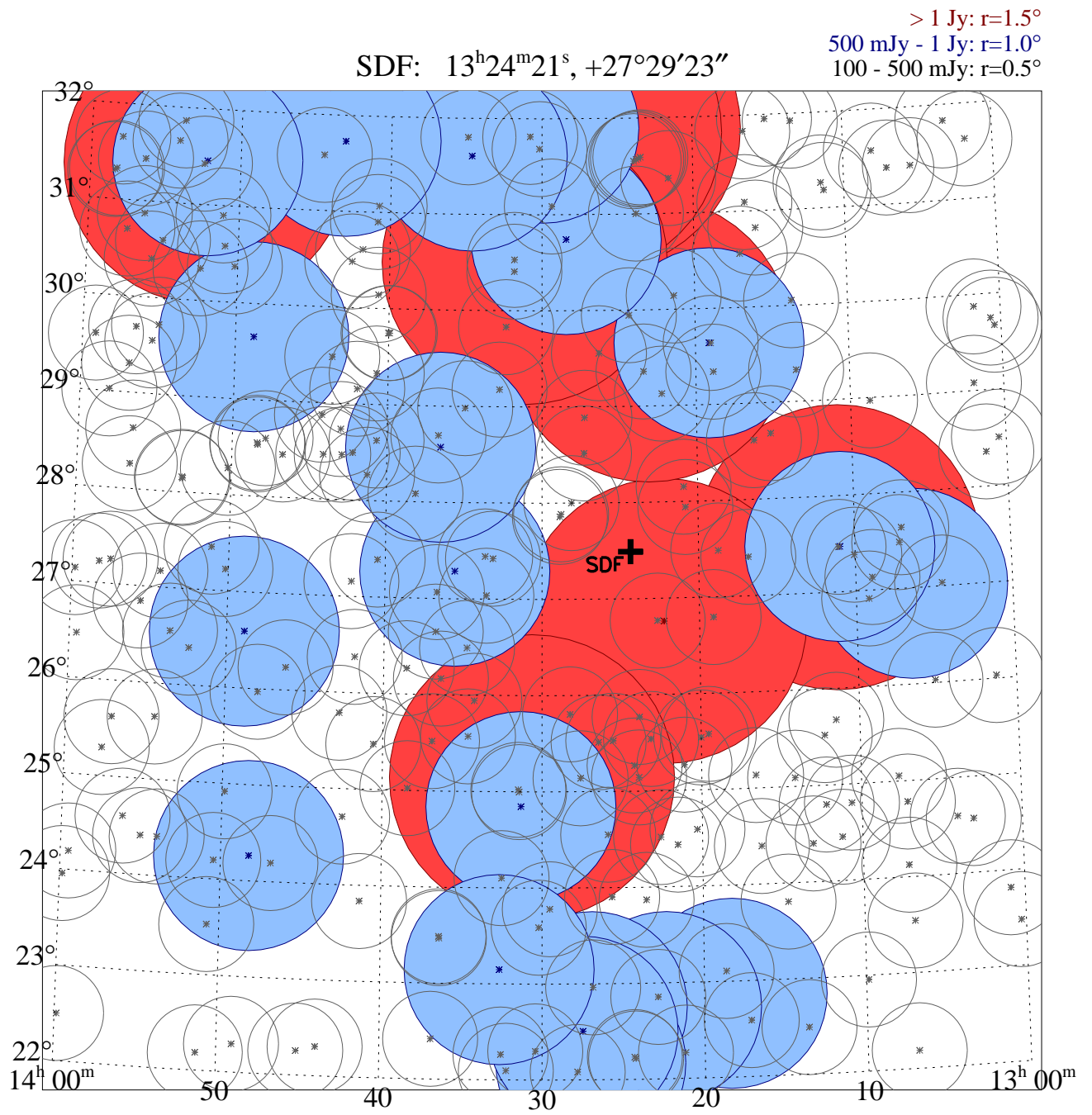


Figure 9: As for Figure 3, but for the SDF.

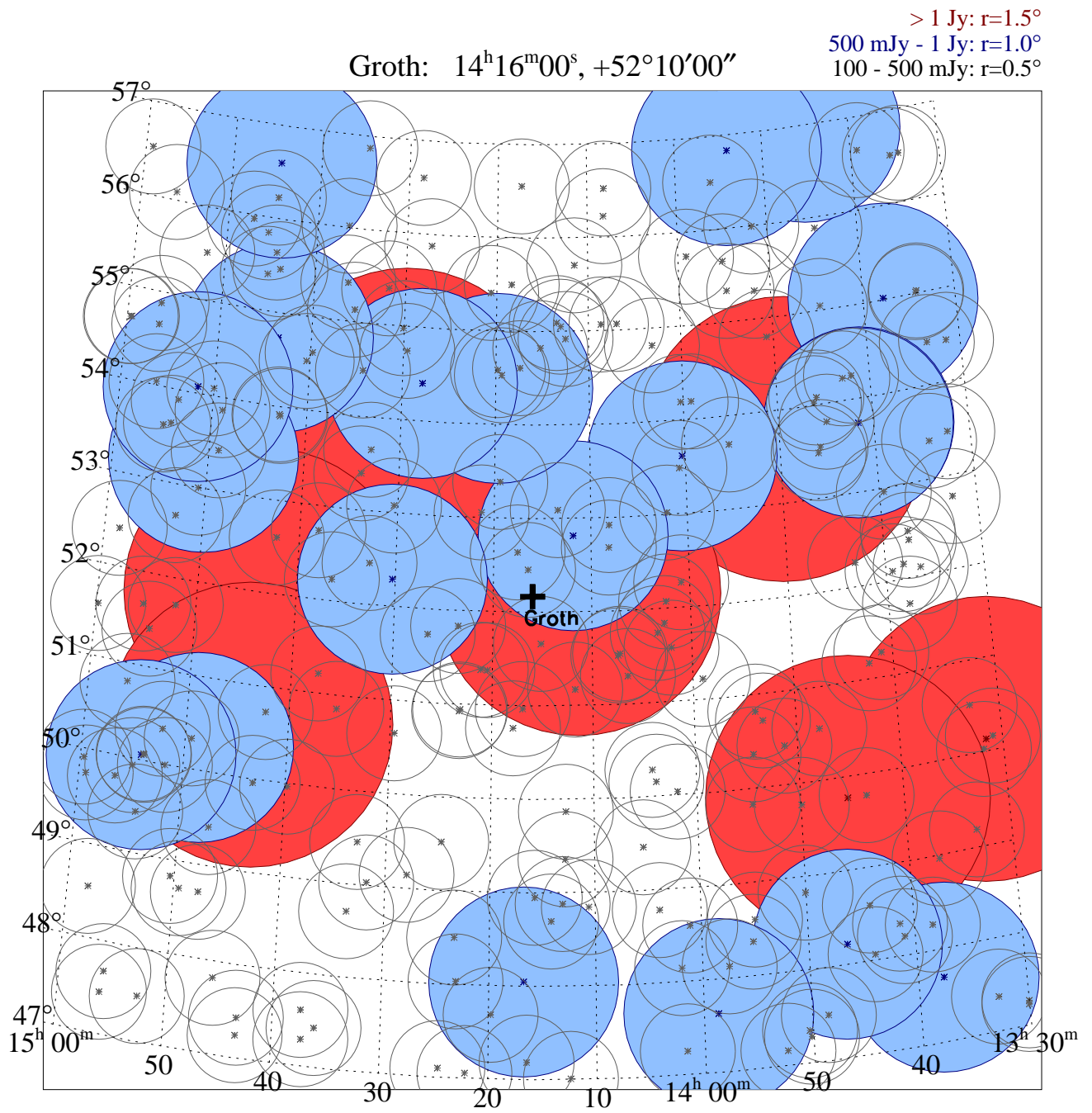


Figure 10: As for Figure 3, but for the Groth strip.

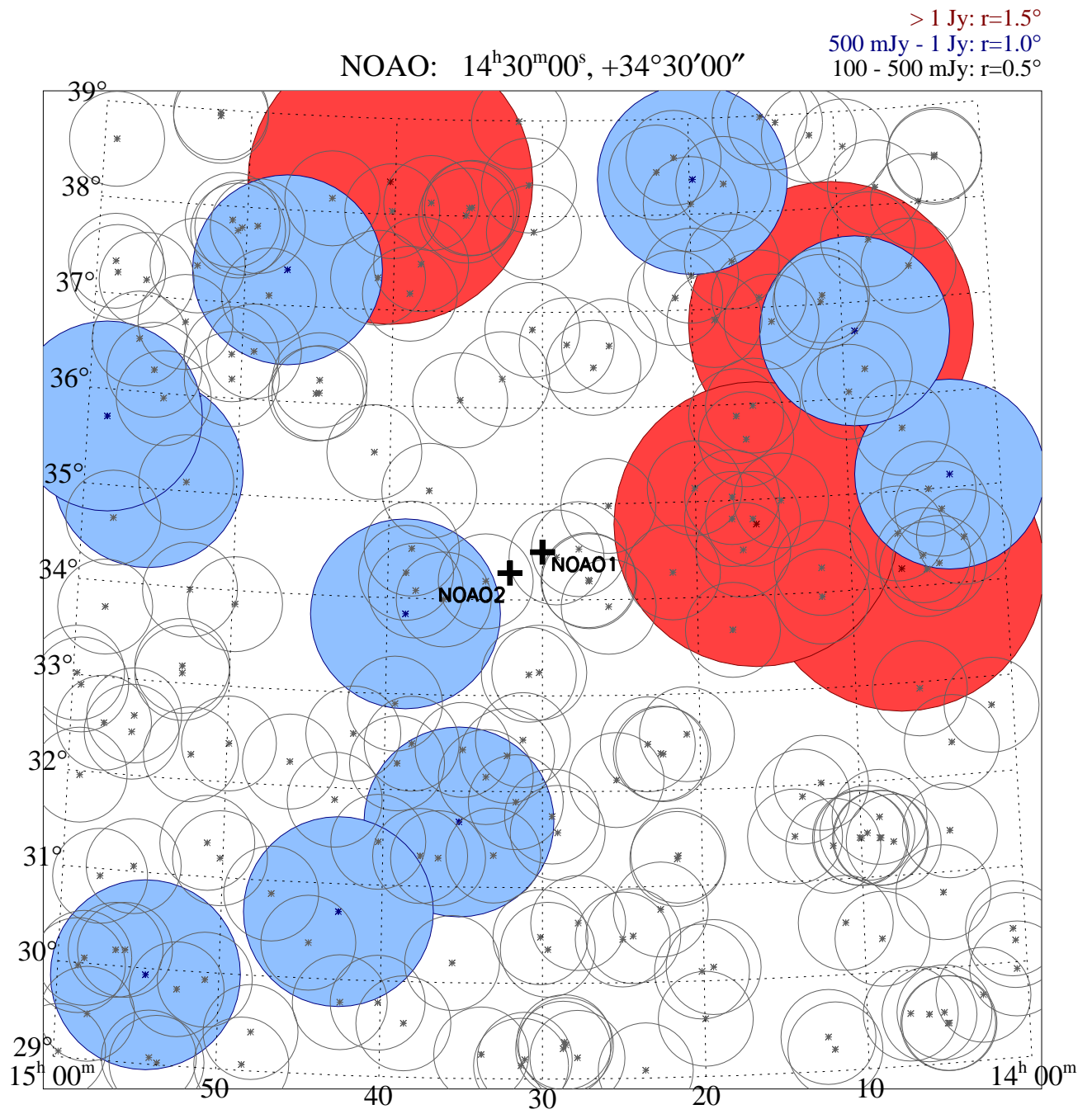


Figure 11: As for Figure 3, but for the NOAO deep field.



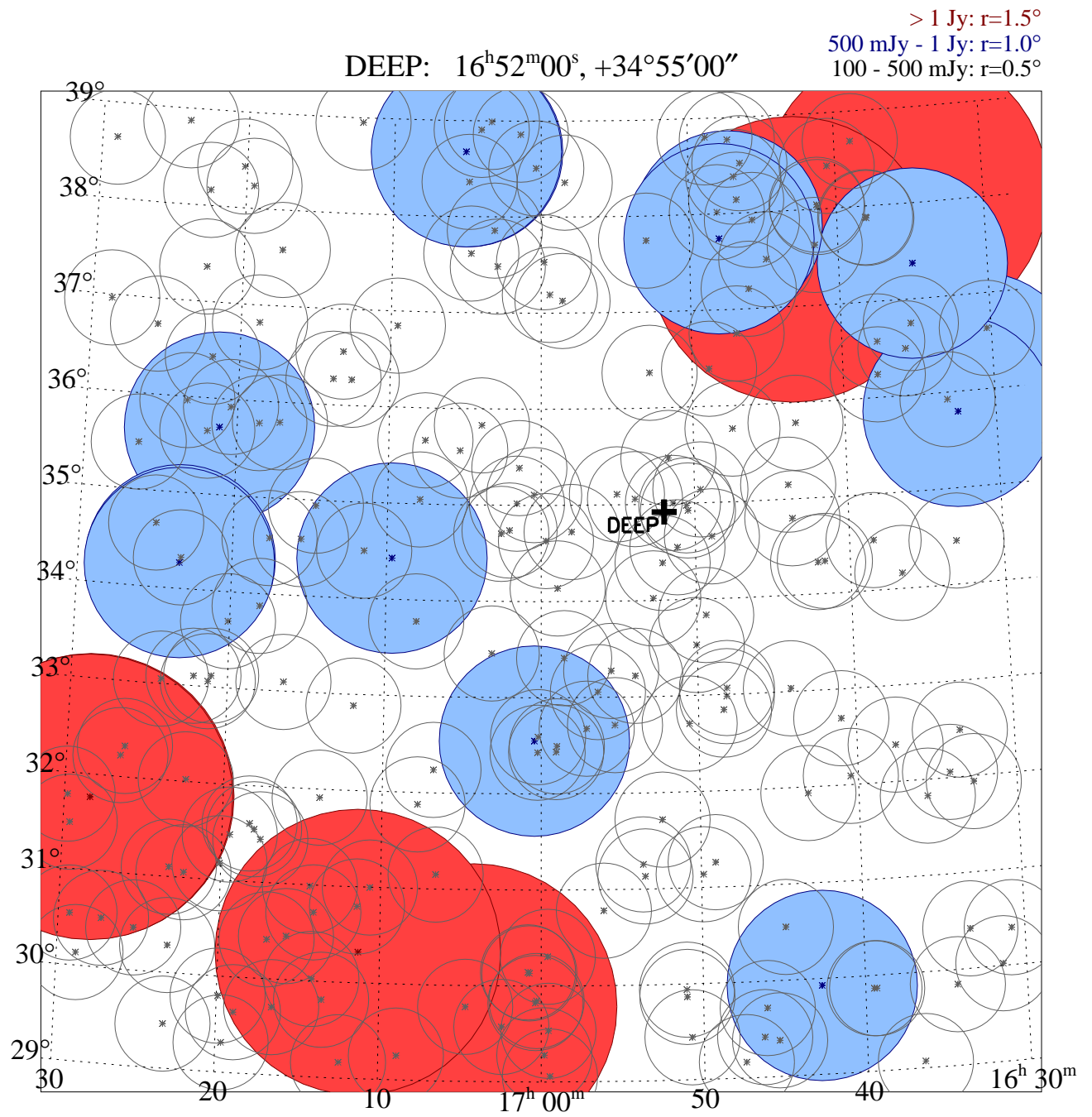


Figure 12: As for Figure 3, but for the DEEP survey area.